

# On Secure Mixed RF-FSO Systems With TAS and Imperfect CSI

Hongjiang Lei, Haolun Luo, Ki-Hong Park, Imran Shafique Ansari,  
Weijia Lei, Gaofeng Pan, and Mohamed-Slim Alouini

## Abstract

In this work, we analyze the secrecy outage performance of a dual-hop relay system composed of multiple-input-multiple-output radio-frequency (RF) links and a free-space optical (FSO) link while a multiple-antenna eavesdropper wiretaps the confidential information by decoding the received signals from the resource node. The channel state information (CSI) of the RF and FSO links is considered to be outdated. We propose three transmit antenna selection (TAS) schemes to enhance the secrecy performance of the considered systems. The secrecy outage performance with different TAS schemes is analyzed and the effects of misalignment and detection technology on the secrecy outage performance of mixed systems are studied. We derive the closed-form expressions for probability density function (PDF) and cumulative distribution function (CDF) over Málaga channel with imperfect CSI. Then the closed-form expressions for the CDF and PDF of the equivalent signal-to-noise ratio (SNR) at the legitimate receiver over Nakagami- $m$  and Málaga channels are derived. Furthermore, the lower bound of the secrecy outage probability (SOP) with different TAS schemes are derived. Besides, the asymptotic results for SOP are investigated by exploiting the unfolding of Meijer's  $G$ -function when the electrical SNR of FSO link approaches infinity. Finally, Monte-Carlo simulation results are presented to testify the correctness of the proposed analysis. The results illustrate that the outdated CSI shows a strong effect on the secrecy outage performance. In addition, increasing the number of antennas at the source cannot significantly enhance the secrecy performance of the considered systems.

Manuscript received.

H. Lei, H. Luo and W. Lei are with School of Communication and Information Engineering, Chongqing University of Posts and Telecommunications, Chongqing 400065, China (e-mail: leihj@cqupt.edu.cn; cquptlhl@gmail.com; leiwj@cqupt.edu.cn).

I. S. Ansari is with the School of Engineering, University of Glasgow, Glasgow G12 8QQ, United Kingdom (Imran.ansari@glasgow.ac.uk).

G. Pan is with Chongqing Key Laboratory of Nonlinear Circuits and Intelligent Information Processing, Southwest University, Chongqing 400715, (e-mail: penngaofeng@qq.com).

K.-H. Park and M.-S. Alouini are with CEMSE Division, King Abdullah University of Science and Technology (KAUST), Thuwal 23955-6900, Saudi Arabia (e-mail: kihong.park@kaust.edu.sa; slim.alouini@kaust.edu.sa).

## Index Terms

Mixed RF-FSO systems, outdated channel state information, physical layer security, secrecy outage probability, transmit antenna selection.

## I. INTRODUCTION

### A. Background and Related Literature

The increase in multimedia services not only leads to increase in the requirements for the transmission rate of communications but also the emergence of communication security [1]. Free space optical (FSO) communications are regarded as a hopeful solution operating in the unlicensed spectrum [2]. It can offer high data rates and be utilized for various applications such as fiber backup, enterprise/local area network connectivity, back-haul for wireless cellular networks, metropolitan area network extensions, redundant link, and disaster recovery. However, inhomogeneities induced by a change of the temperature and atmospheric pressure cause fluctuations in the refractive index. This impairment caused by the atmospheric effects is known as atmospheric turbulence.

Relaying is a state-of-the-art technology that has been widely utilized in wireless communication [3], [4]. By utilizing relaying technology, the mixed radio frequency (RF)-FSO systems combine both the advantages of the RF and FSO communication technologies. The common performance of mixed RF-FSO systems was analyzed and the closed-form expressions for outage probability (OP), average symbol error rate (ASER), and ergodic capacity (EC) were derived vastly in the open literature (See the Table I in [5]). In addition, mixed RF-FSO systems with multiple antennas or multiple users have been analyzed in many works [6] - [10]. For example, the common performance of mixed multiple-input single-output (MISO) RF-FSO systems was investigated in [6]. Varshney *et al.* analyzed cognitive multiple-input-multiple-output (MIMO) RF-FSO systems with perfect and imperfect channel state information (CSI) in [7], [8], and [9], respectively. Moreover, the performance of mixed RF-FSO systems with opportunistic scheduling scheme was investigated in [10].

As stated in many literature [11]-[17], it is impossible to obtain the perfect CSI for wireless links in practical systems, including RF and FSO links. The obtained CSI at source node is always outdated (due to delay) or imperfect (with estimation errors). The performance of RF systems with outdated CSI was investigated in many literatures, such as [11]-[17]. The mixed

RF-FSO systems with imperfect CSI was considered in many works, such as [18] - [23]. The performance of a mixed RF-FSO decode-and-forward (DF) cooperative system was analyzed in [18] where MIMO with zero-forcing based linear receiver was employed over RF links. Salhab investigated the performance of a multiuser mixed RF-FSO relay network with generalized order user scheduling and obtained the closed-form expressions for OP, average bit error rate (ABER), and EC in [19]. Then a power allocation scheme was proposed to optimize the performance of the multiuser mixed RF-FSO system in [20]. The performance of mixed dual-hop RF-FSO system is analysed while variable gain relaying scheme was utilized at relay node and the closed-form expressions for OP and ABER were derived in [21]. Petkovic *et al.* analyzed the common performance of a dual-hop mixed RF-FSO system with partial amplify-and-forward (AF) relay selection scheme and derived the closed-form expressions for OP and ABER in [22]. A similar system was analyzed in [23] wherein both AF and DF schemes were considered and the FSO link was assumed to follow Málaga distribution. It must be noted that in [18] - [23], the outdated CSI of RF links was considered and the CSI of FSO links was assumed to be perfect. Furthermore, only the common performance metrics were investigated.

Physical layer security has been regarded as a prospective solution for wireless communications through utilizing the inherent randomness of wireless medium [24] - [27]. Recently, the physical layer security of mixed RF-FSO systems was investigated in many works. El-Malek *et al.* analyzed the security reliability trade-off (SRT) of a multiuser mixed RF-FSO system in [28] and derived the closed-form expressions for OP, ASER, EC, and intercept probability. The effect on SRT of multiuser mixed RF-FSO systems from RF cochannel interference was analyzed in [29] and a power allocation scheme was proposed to enhance the secrecy performance of the considered system. In previous work [30], we analyzed the secrecy performance of the mixed RF-FSO uplink system wherein the closed-form expressions for secrecy outage probability (SOP) and ergodic secrecy capacity were derived under different relaying schemes and detection techniques. The secrecy outage performance of a mixed RF-FSO downlink systems was analyzed in [31] where energy harvesting technology was utilized in RF links. We derived the expressions for the exact and asymptotic SOPs and discussed the effects of atmospheric turbulence, pointing error, detection technology, path loss, and energy harvesting on secrecy performance.

To the best of the authors' knowledge, no open literature addresses the performance of FSO systems with imperfect CSI except [32]. The common performance of FSO systems with imprecise channel models was analyzed and the closed-form expressions for the OP, ABER, and

EC were derived in [32]. The atmospheric fading over FSO links was characterized by Gamma-Gamma turbulence model and only intensity modulation/direct detection (IM/DD) technology was considered. Based on the results in [32], the secrecy outage performance of a mixed single-input multiple-output (SIMO) RF-FSO system was analyzed in [33] and the imperfect CSI of both RF and FSO links was considered. But the RF and FSO links are modeled as Rayleigh and Gamma-Gamma channel, respectively.

### B. Motivation and Contributions

Málaga distribution is the most generalized statistical model that describes the effect of irradiance fluctuation over FSO link. It includes many other fading models for atmospheric optical communications, such as Log-Normal, Gamma-Gamma, Gamma-Rician, Shadowed-Rician, *etc.* as its special cases [34]. Table I in [34] lists the relationship between these existing distribution models and Málaga distribution. There are some works that have analyzed the common performance of FSO links or mixed RF-FSO systems over Málaga distribution, such as [6], [10], [35], respectively. But all these works assume a perfect CSI scenario.

Transmit antenna selection (TAS) scheme has been verified as an effective scheme to enhance the secrecy performance of wireless communications [15], [36] - [39]. In this paper, three TAS schemes are proposed to improve the secrecy performance of mixed systems with imperfect CSI. The main contributions of this article are:

- Differing from [32], we analyze the statistical characteristics of Málaga fading channels with imperfect CSI under heterodyne detection (HD) and IM/DD techniques in presence of pointing errors. The closed-form expressions for the probability density function (PDF) and cumulative distribution function (CDF) are obtained. To the best of author's knowledge based on the open literature, the results are new to the literature. One can easily utilize these to investigate the common performance metrics of FSO systems over Málaga fading channels.
- Further, three different TAS schemes are proposed to enhance the secrecy performance of mixed RF-FSO systems. The secrecy outage performance of these schemes is analyzed and compared with the optimal TAS (OTAS) scheme. We derive the closed-form expressions for the exact and asymptotic SOP for different TAS schemes. Moreover, Monte-Carlo simulation results are demonstrated to validate the accuracy of our analytical results.

- Differing from [7], in which the TAS scheme was utilized to enhance the common performance while reducing the hardware complexity, in this work, we propose three different TAS schemes to improve the secrecy performance while the imperfect CSI of both RF and FSO links are considered.
- Differing from [18] - [23], we consider the outdated CSI for both RF and FSO links in this work wherein the respective secrecy performance is investigated. Technically speaking, it is much more challenging to analyze the secrecy performance relative to the common performance metrics, especially under the influence of imperfect CSI.
- Differing from [30], the system in this work is more practical since both RF and FSO links are considered with imperfect CSI. The source, relay, and eavesdropper are equipped with multiple antennas. Differing from [33], the system in this work is generalized since the FSO link is assumed to follow Málaga distribution. Moreover, several TAS schemes are proposed to improve the secrecy performance of mixed RF-FSO systems.

### C. Structure

The remainder of this work is organized as follows. In Section II, we present the mixed RF-FSO system model and the statistical characteristics of each link are presented. The expressions of secrecy outage performance and its asymptotic results for different TAS schemes are obtained in Section III. Monte-Carlo simulation and numerical results are presented in Section IV. Finally, we conclude the work in Section V.

## II. SYSTEM MODEL AND STATISTICAL ANALYSIS

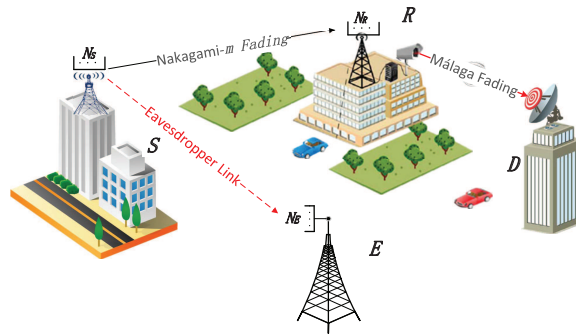


Fig. 1. System model depicting the source ( $S$ ), relay ( $R$ ), destination ( $D$ ), and eavesdropper ( $E$ ) along with their respective antennas and links between them. The CSI of RF links are outdated and the CSI estimation of the FSO link is imperfect.

Fig. 1 shows a dual-hop mixed relay system composed of MIMO RF links and an FSO link. A source node ( $S$ ) transmits the confidential information to a destination ( $D$ ) with the help of an intermediate relay ( $R$ ), while a multiple-antenna eavesdropper ( $E$ ) wiretaps the confidential information by decoding the received signals. It is noteworthy that  $E$  can not receive any signals from  $R$  since the FSO link is secure due to the high directionality of laser beam [28], [29], [30], [33]. It is assumed that  $S$ ,  $R$ , and  $E$  are equipped with  $N_i$  ( $i \in \{S, R, E\}$ ) multiple antennas, respectively. TAS scheme is utilized at  $S$  since it makes full use of the advantages of MIMO system. Maximal ratio combining (MRC) scheme is utilized at both  $R$  and  $E$  to improve the received signal-to-noise ratio (SNR). The RF links experience Nakagami- $m$  with parameter  $m_i$  ( $i \in \{R, E\}$ ) wherein the CSI are outdated and the FSO link follows Málaga fading wherein the CSI estimation is imperfect.

#### A. FSO Link with Imperfect CSI

The outdated FSO link channel gain  $\hat{h}_{RD}$  is expressed as [32]

$$\hat{h}_{RD} = \rho_{\text{FSO}} h_{RD} + \sqrt{1 - \rho_{\text{FSO}}^2} \varepsilon, \quad (1)$$

where  $h_{RD}$  is the accurate channel gain of  $R$ - $D$  link, which is modeled as Málaga channel,  $\varepsilon$  is a Gaussian random variable that has zero-mean and unit variance and is independent of  $h_{RD}$ , and  $\rho_{\text{FSO}}$  denotes the correlation coefficient. The instantaneous SNR of FSO link can be expressed as [35]

$$\hat{\gamma}_{RD} = \bar{\gamma}_{RD} \hat{h}_{RD}^r, \quad (2)$$

where  $\bar{\gamma}_{RD}$  is the electrical SNR of FSO link,  $r$  is the parameter that represents the type of detection technology being utilized, i.e.  $r = 1$  accounts for HD and  $r = 2$  represents IM/DD.

*Lemma 1:* The PDF and CDF of  $\hat{\gamma}_{RD}$  are obtained as

$$f_{\hat{\gamma}_{RD}}(\gamma) = \begin{cases} B_D \sum_{h=1}^{\beta} \sum_{k=0}^{\infty} b_h \varphi_1 e^{-\psi_1 \gamma^{\frac{2}{r}}} \gamma^{\frac{k+1}{r}-1}, & \gamma > 0 \\ 1 - Z_0, & \gamma = 0 \end{cases} \quad (3)$$

$$F_{\hat{\gamma}_{RD}}(\gamma) = \begin{cases} B_D \sum_{h=1}^{\beta} \sum_{k=0}^{\infty} H_1 G_{1,2}^{1,1} \left[ \psi_1 \gamma^{\frac{2}{r}} \left| \frac{1+k}{2}, 0 \right. \right], & \gamma > 0 \\ 1 - Z_0, & \gamma = 0 \end{cases} \quad (4)$$

respectively, where  $B_D = \frac{\xi^2 A_D 2^{\alpha-4.5}}{\pi^{1.5}}$ ,  $A_D = \frac{2\alpha^{0.5\alpha}}{g^{1+0.5\alpha}\Gamma(\alpha)} \left(\frac{g\beta}{g\beta+\Omega_1}\right)^{\beta+0.5\alpha}$ ,  $\varphi_1 = \frac{2^{0.5k+h} G_k}{rk! \bar{\gamma}_{RD}^{1+k} (1-\rho_{FSO}^2)^{0.5(k+1)}}$ ,  $b_h = \frac{(\beta-1)!(g\beta+\Omega_1)^{1-0.5h} \alpha^{0.5h} \Omega_1^{h-1}}{((h-1)!)^2 (\beta-h)! \beta^{0.5h} g^{h-1}} \left(\frac{\alpha\beta}{g\beta+\Omega_1}\right)^{-0.5(\alpha+h)}$ ,  $\psi_1 = \frac{1}{2\bar{\gamma}_{RD}^{\frac{r}{2}} (1-\rho_{FSO}^2)}$ ,  $H_1 = \frac{b_h 2^{k+h-0.5} G_k}{k!}$ ,  $Z_0 = \frac{\xi^2 A_D}{\pi^{1.5}} \sum_{h=1}^{\beta} \sum_{k=0}^{\infty} \frac{2^{k+\alpha+h-5} b_h G_k}{k!} \Gamma\left(\frac{k+1}{2}\right)$ ,  $\Gamma(\cdot)$  is the Gamma function, as defined by eq. (8.310) of [40],  $\alpha$  and  $\beta$  are fading parameters,  $g = 2b_0(1-\rho_0)$  denotes the average power of the scattering component received by off-axis eddies,  $2b_0$  is the average power of the total scatter components,  $\rho_0$  represents the amount of scattering power coupled to the line-of-sight (LOS) component,  $\Omega_1 = \Omega + 2b_0\rho_0 + 2\sqrt{2b_0\rho_0}\Omega \cos(\varphi_A - \varphi_B)$  represents the average power from the coherent contributions,  $\Omega$  is the average power of the LOS component,  $\varphi_A$  and  $\varphi_B$  are the deterministic phases of the LOS and the coupled-to-LOS scatter terms, respectively.  $G_k = G_{6,3}^{1,6} \left[ \frac{2^3}{\delta^2(1-\rho_{FSO}^2)} \left| \begin{matrix} \frac{1-\xi^2}{2}, \frac{2-\xi^2}{2}, \frac{1-\alpha}{2}, \frac{2-\alpha}{2}, \frac{1-h}{2}, \frac{2-h}{2} \\ \frac{k}{2}, \frac{-\xi^2}{2}, \frac{1-\xi^2}{2} \end{matrix} \right. \right]$ , where  $\delta = \frac{\alpha\beta}{(g\beta+\Omega_1)I_l A_0 \rho_{FSO}}$ ,  $I_l$  is the path loss that is a constant in a given weather condition,  $A_0$  and  $\xi$  are constants term that defines the pointing loss, and  $G_{p,q}^{m,n}[\cdot]$  is the Meijer's  $G$ -function as defined by Eq.(9.301) of [40].

*Proof*: See Appendix A.

*Remark 1*: Table I in [34] lists many existing distribution models that can be utilized for atmospheric optical communications and how these models can be generated from the Málaga distribution model. Thus one can easily obtain the PDF and CDF for all these models with imprecise CSI. For instance, when  $\rho_0 = 1$ ,  $\Omega_1 = 1$ ,  $r = 1$ , the CDF presented in (4) agrees with the individual result presented by (23) (for  $\xi \rightarrow \infty$ ) and (24) of [32], respectively. Based on the results in this work and making use of the method proposed in [41] and [42], one can easily analyze the common performance metrics of the corresponding systems over Málaga distribution with imperfect CSI, such as OP, ABER/ASER, and EC.

## B. TAS Based On S-R Link

In proactive eavesdropping scenarios where the eavesdropper's CSI is unknown for  $S$ , one can select antenna based on the CSI of  $S$ - $R$  links. The TAS criterion of this scheme (TASR) can be expressed as

$$b_1 = \arg \max_{1 \leq i \leq N_S} \left( \sum_{j=1}^{N_R} |h_{S_i R_j}|^2 \right), \quad (5)$$

where  $b_1$  signifies the selected antenna at  $S$  with this scheme. Thus the SNR at  $R$  can be written as

$$\hat{\gamma}_{SR,1} = \frac{P_S}{N_0} \sum_{j=1}^{N_R} \left| \hat{h}_{S_{b_1}R_j} \right|^2, \quad (6)$$

where  $P_S$  is the transmit power at  $S$  and  $N_0$  denotes the variance of additive white Gaussian noise (AWGN).

The correlation relationship between the outdated and accurate channel gain can be expressed as [11]

$$\hat{h}_{S_iR_j} = \rho_{SR} h_{S_iR_j} + \sqrt{1 - \rho_{SR}^2} \omega_1, \quad (7)$$

where  $\hat{h}_{S_iR_j}$  and  $h_{S_iR_j}$  are the outdated and accurate channel gain between the  $i$ -th antenna at  $S$  and  $j$ -th antenna at  $R$ , respectively,  $\omega_1$  represents a Nakagami- $m$  random variable with same variance as  $h_{S_iR_j}$ , and  $0 < \rho_{SR} < 1$  is the correlation coefficient.

*Lemma 2:* The PDF and CDF of  $\hat{\gamma}_{SR,1}$  can be expressed as

$$f_{\hat{\gamma}_{SR,1}}(\gamma) = \phi_R \sum_{S_R} \sum_{q=0}^{B_R} \Lambda_R \gamma^{q+\tau_R-1} e^{-v_R \gamma}, \quad (8)$$

$$F_{\hat{\gamma}_{SR,1}}(\gamma) = 1 - \phi_R \sum_{S_R} \sum_{q=0}^{B_R} \sum_{t=0}^{q+\tau_R-1} \varphi_R \gamma^t e^{-v_R \gamma}, \quad (9)$$

respectively, where  $\phi_R = \frac{N_S \lambda_R^{\tau_R+1} \rho_{SR}^{1-\tau_R}}{(1-\rho_{SR}^2) \Gamma(\tau_R)}$ ,  $\tau_R = N_R m_R$ ,  $\lambda_R = \frac{m_R}{\bar{\gamma}_{SR}}$ ,  $B_R = \sum_{p=2}^{\tau_R+1} n_p (p-2)$ ,

$S_R = \left\{ (n_1, \dots, n_{\tau_R+1}) \in \mathbb{N} \left| \sum_{p=1}^{\tau_R+1} n_p = N_S - 1 \right. \right\}$ ,  $\mathbb{N}$  denotes a non-negative integer set,  $v_R =$

$\frac{\lambda_R}{1-\rho_{SR}^2} - \frac{(\lambda_R \beta_R)^2}{\alpha_R}$ ,  $\Lambda_R = \frac{A_R B_R! (\lambda_R \beta_R)^{2q+\tau_R-1} (B_R+\tau_R-1)!}{q! \alpha_R^{B_R+\tau_R+q} (B_R-q)! (\tau_R+q-1)!}$ ,  $\varphi_R = \frac{\Lambda_R (q+\tau_R-1)! v_R^{t-q-\tau_R}}{t!}$ ,  $\beta_R = \frac{\rho_{SR}^2}{1-\rho_{SR}^2}$ ,

$A_R = \left( \frac{N_S-1}{\prod_{q=1}^{\tau_R+1} n_q} \right) \prod_{p=2}^{\tau_R+1} \left( -\frac{\lambda_R^{p-2}}{(p-2)!} \right)^{n_p}$ ,  $\alpha_R = \lambda_R \left( \frac{\rho_{SR}^2}{1-\rho_{SR}^2} + C_R + 1 \right)$ ,  $C_R = \sum_{p=2}^{\tau_R+1} n_p$ , and  $\bar{\gamma}_{SR}$  is the

average SNR of  $S-R$  link.

*Proof:* See Appendix B.

It is assumed that DF relaying scheme is utilized at  $R$ . Then the equivalent SNR at  $D$  can be



expressed as <sup>1</sup>

$$\gamma_{eq} = \min(\hat{\gamma}_{SR,1}, \hat{\gamma}_{RD}). \quad (10)$$

Then the CDF of  $\gamma_{eq}$  in this case is obtained as

$$\begin{aligned} F_{\gamma_{eq,1}}(\gamma) &= F_{\hat{\gamma}_{SR}}(\gamma) + F_{\hat{\gamma}_{RD}}(\gamma) - F_{\hat{\gamma}_{SR}}(\gamma)F_{\hat{\gamma}_{RD}}(\gamma) \\ &= 1 + \phi_R \sum_{S_R} \sum_{q=0}^{B_R} \sum_{t=0}^{q+\tau_R-1} \varphi_R \gamma^t e^{-\nu_R \gamma} \left( B_D \sum_{h=1}^{\beta} \sum_{k=0}^{\infty} H_1 G_{1,2}^{1,1} \left[ \psi_1 \gamma^{\frac{2}{r}} \left| \begin{matrix} 1 \\ \frac{1+k}{2}, 0 \end{matrix} \right. \right] - Z_0 \right). \end{aligned} \quad (11)$$

*Remark 2:* It should be noted that there are two main differences between (1) and (7), although they are expressed in similar expression. Firstly,  $\hat{h}_{RD}$  must be positive real value while  $\hat{h}_{S_i R_j}$  can be any complex value. Secondly,  $\varepsilon$  signifies the channel estimation errors while  $\omega_1$  represents the errors from being outdated. For the case that  $N_S = 1$ ,  $\omega_1$  will not influence  $\hat{h}_{S_i R_j}$  since there is no antenna selection. The effect of estimation errors in both RF and FSO links on the secrecy performance of mixed systems was investigated in [33]. In this work, we analyzed the influence of the outdated CSI of RF link and estimation errors in FSO link on security of mixed systems. Considering the estimation errors along with being outdated under TAS is an interesting work and will be addressed in our future work.

TAS is based on the CSI of  $S$ - $R$  link, which means a random transmit antenna would be selected for  $E$  [36]. Then the SNR at  $E$  in this case can be expressed as

$$\gamma_{SE,1} = \frac{P_S}{N_0} \sum_{j=1}^{N_E} \left| h_{S_{b_1} E_j} \right|^2. \quad (12)$$

The PDF and CDF of  $\gamma_{SE,1}$  are given by [36]

$$f_{\gamma_{SE,1}}(x) = \frac{\lambda_E^{\tau_E}}{\Gamma(\tau_E)} e^{-\lambda_E x} x^{\tau_E-1}, \quad (13)$$

$$F_{\gamma_{SE,1}}(x) = 1 - \sum_{i=0}^{\tau_E-1} \frac{e^{-\lambda_E x}}{i!} (\lambda_E x)^i, \quad (14)$$

where  $\lambda_E = \frac{m_E}{\bar{\gamma}_{SE}}$ ,  $\tau_E = m_E N_E$ , and  $\bar{\gamma}_{SE}$  is the average SNR of  $S$  -  $E$  link.

<sup>1</sup>The results are also fit to the bound of variable gain amplify-and-forward relaying scheme, as testified in vast existing literature, such as [30], [33], [41], [42].

### C. TAS Based On $S$ - $E$ Link

In the active eavesdropping scenario wherein the CSI of eavesdropping link is available at  $S$ <sup>2</sup>, the antenna can be selected based on the CSI of  $S$ - $E$  links, the TAS criterion in this scheme (TASE) can be expressed as

$$b_2 = \arg \min_{1 \leq i \leq N_E} \left( \sum_{j=1}^{N_R} |h_{S_i E_j}|^2 \right), \quad (15)$$

where  $b_2$  signifies the selected antenna at  $S$  based on  $S$ - $E$  link. Thus the SNR at  $E$  can be written as

$$\hat{\gamma}_{SE,2} = \frac{P_S}{N_0} \sum_{j=1}^{N_E} \left| \hat{h}_{S_{b_2} E_j} \right|^2. \quad (16)$$

Similarly, we have

$$\hat{h}_{S_i E_j} = \rho_{SE} h_{S_i E_j} + \sqrt{1 - \rho_{SE}^2} \omega_2, \quad (17)$$

where  $\hat{h}_{S_i E_j}$  and  $h_{S_i E_j}$  are the outdated and accurate channel gain between the  $i$ -th antenna at  $S$  and  $j$ -th antenna at  $E$ , respectively,  $\omega_2$  represents a Nakagami- $m$  random variable with same variance as  $h_{S_i E_j}$ , and  $0 < \rho_{SE} < 1$  is the correlation coefficient.

*Lemma 3:* The PDF and CDF of  $\hat{\gamma}_{SE,2}$  are given as

$$f_{\hat{\gamma}_{SE,2}}(\gamma) = \phi_E \sum_{S_E} \sum_{q=0}^{B_E} \Lambda_E \gamma^{q+\tau_E-1} e^{-\nu_E \gamma}, \quad (18)$$

$$F_{\hat{\gamma}_{SE,2}}(x) = 1 - \phi_E \sum_{S_E} \sum_{q=0}^{B_E} \sum_{t=0}^{q+\tau_E-1} \varphi_E x^t e^{-\nu_E x}, \quad (19)$$

respectively, where  $\phi_E = \frac{N_S \lambda_E^{\tau_E+1} \rho_{SE}^{1-\tau_E}}{\Gamma(\tau_E)(1-\rho_{SE}^2)}$ ,  $S_E = \left\{ (n_1, \dots, n_{\tau_E}) \in \mathbb{Z}^{\geq} \left| \sum_{p=1}^{\tau_E} n_p = N_S - 1 \right. \right\}$ ,  $\beta_E = \frac{\rho_{SE}^2}{1-\rho_{SE}^2}$ ,  $\nu_E = \frac{\lambda_E}{1-\rho_{SE}^2} - \frac{(\lambda_E \beta_E)^2}{\alpha_E}$ ,  $\varphi_E = \frac{\Lambda_E (q+\tau_E-1)! \nu_E^{t-q-\tau_E}}{t!}$ ,  $\alpha_E = \lambda_E \left( \frac{\rho_{SE}^2}{1-\rho_{SE}^2} + C_E + 1 \right)$ ,  $A_E = \left( \frac{N_S-1}{\tau_E} \prod_{q=1}^{\tau_E} n_q \right) \prod_{p=1}^{\tau_E} \left( \frac{\lambda_E^{p-1}}{(p-1)!} \right)^{n_p}$ ,  $B_E = \sum_{p=1}^{\tau_E} n_p (p-1)$ ,  $C_E = \sum_{p=1}^{\tau_E} n_p$ , and  $\Lambda_E = \frac{A_E B_E! (\lambda_E \beta_E)^{2q+\tau_E-1} (B_E+\tau_E-1)!}{q! \alpha_E^{B_E+\tau_E+q} (B_E-q)! (\tau_E+q-1)!}$ .

*Proof:* See Appendix C.

<sup>2</sup>The CSI of the eavesdropping links can be estimated and obtained by monitoring the eavesdropper transmissions, which have been introduced in [24] and [43].

Similarly, TAS based on the CSI of  $S$ - $E$  link signifies that a random transmit antenna would be selected for  $R$ . Thus the SNR at  $R$  under this scheme can be expressed as

$$\gamma_{SR,2} = \frac{P_S}{N_0} \sum_{j=1}^{N_R} |h_{Sb_2R_j}|^2. \quad (20)$$

The PDF and CDF of  $\gamma_{SR,2}$  can be easily obtained as

$$f_{\gamma_{SR,2}}(x) = \frac{\lambda_R^{\tau_R}}{\Gamma(\tau_R)} e^{-\lambda_R x} x^{\tau_R-1}, \quad (21)$$

$$F_{\gamma_{SR,2}}(x) = 1 - \sum_{i=0}^{\tau_R-1} \frac{e^{-\lambda_R x}}{i!} (\lambda_R x)^i. \quad (22)$$

Finally, we obtain the CDF of  $\gamma_{eq}$  in this case as

$$\begin{aligned} F_{\gamma_{eq,2}}(\gamma) &= F_{\gamma_{SR,2}}(\gamma) + F_{\hat{\gamma}_{RD}}(\gamma) - F_{\gamma_{SR,2}}(\gamma) F_{\hat{\gamma}_{RD}}(\gamma) \\ &= 1 + \sum_{i=0}^{\tau_R-1} \frac{e^{-\lambda_R \gamma}}{i!} (\lambda_R \gamma)^i \left( B_D \sum_{h=1}^{\beta} \sum_{k=0}^{\infty} H_1 G_{1,2}^{1,1} \left[ \psi_1 \gamma^{\frac{2}{r}} \left| \frac{1+k}{2}, 0 \right. \right] - Z_0 \right). \end{aligned} \quad (23)$$

*Remark 3:* Based on (10), one can observe that when  $\hat{\gamma}_{SR} > \hat{\gamma}_{RD}$ , which means the FSO link is the bottleneck of the equivalent SNR at the destination, the TAS based on  $S$ - $E$  link will be the optimal TAS scheme because SOP in this case is independent of  $S$ - $R$  links.

*Remark 4:* There is another interesting question: when  $\hat{\gamma}_{SR} < \hat{\gamma}_{RD}$ , between the TAS scheme based on  $S$ - $R$  links or  $S$ - $E$  links, which one can obtain better secrecy performance? The answer depends on the relationship between the SNRs of  $S$ - $R$  and  $S$ - $E$  links.

### III. SECRECY OUTAGE PROBABILITY ANALYSIS

The SOP is given as [24]

$$\begin{aligned} P_{out}(R_s) &= \Pr \{C_s(\gamma_{eq}, \gamma_{SE}) \leq R_s\} \\ &= \Pr \{ \gamma_{eq} \leq \Theta \gamma_{SE} + \Theta - 1 \} \\ &= \int_0^{\infty} F_{eq}(\Theta \gamma_{SE} + \Theta - 1) f_{\gamma_{SE}}(\gamma_{SE}) d\gamma_{SE}, \end{aligned} \quad (24)$$

where  $R_s$  signifies the target secrecy capacity threshold and  $\Theta = 2^{R_s}$ . It must be noted that there is a Meijer's  $G$ -function presented in the CDF of FSO link, and hence obtaining a closed-form result for the integral including the shift in the Meijer's  $G$ -function is almost impossible and/or

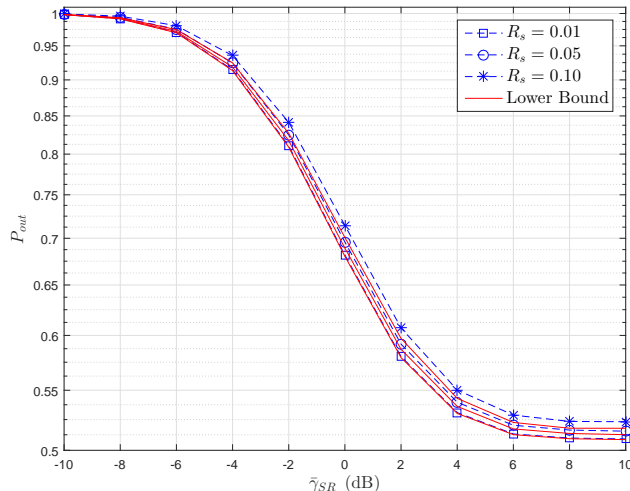


Fig. 2. Simulation results of exact SOP and lower bound for various  $R_s$  with  $N_S = N_R = N_E = 2$ ,  $\alpha = 2.296$ ,  $\beta = 2$ ,  $\xi = 6.7$ ,  $r = 2$ ,  $\rho_{RF} = \rho_{FSO} = 0.7$ ,  $m = 2$ ,  $\bar{\gamma}_{SD} = 5$  dB, and  $\bar{\gamma}_{SE} = 0$  dB.

too complex. Therefore in the subsequent section, the lower bound of the SOP is considered, which has been utilized in many works [30], [33].

$$\begin{aligned}
 P_{out}^L &= \Pr \{ \gamma_{eq} \leq \Theta \gamma_{SE} \} \\
 &= \int_0^\infty F_{eq}(\Theta \gamma_{SE}) f_{\gamma_{SE}}(\gamma_{SE}) d\gamma_{SE}.
 \end{aligned} \tag{25}$$

**About the lower bound:** Compared with (24) and (25), one can find that the tightness between the exact SOP and lower bound for SOP depend on  $\Theta = 2^{R_s}$  and  $\gamma_{SE}$ . We can easily observe that the smaller  $R_s$  and/or larger  $\bar{\gamma}_{SE}$ , the tighter bound. Figs. 2 and 3 represent the simulation results gap between the exact and lower bound for various  $R_s$  and  $\bar{\gamma}_{SE}$ , respectively.

#### A. SOP with the Optimal Transmit Antenna Selection

In the scenario where the source node has the CSI of all the links, the antenna can be selected appropriately in order to maximize the secrecy performance of the mixed RF-FSO system. Based on the results in [36], the criterion of this scheme (OTAS) can be expressed as

$$b_{OTAS} = \arg \max_{1 \leq i \leq N_S} (C_{s,i}^{OTAS}), \tag{26}$$

where  $C_{s,i}^{OTAS} = \log \left( \frac{1 + \min(\gamma_{S_i R}, \hat{\gamma}_{RD})}{1 + \gamma_{S_i E}} \right)$  signifies the secrecy capacity of a mixed RF-FSO system when the  $i$ -th antenna at  $S$  is selected.

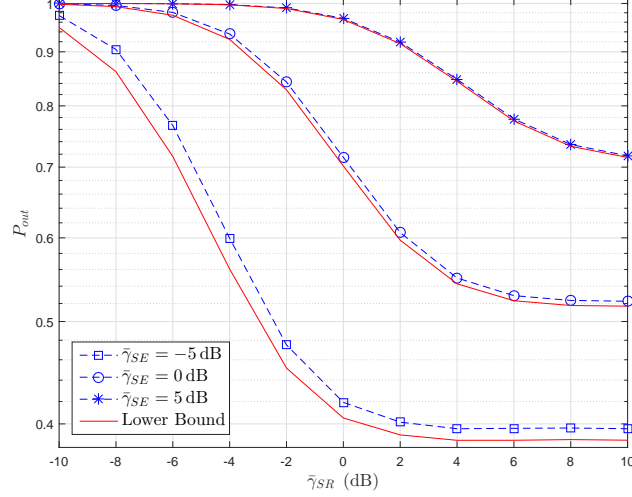


Fig. 3. Simulation results of exact SOP and lower bound for various  $\bar{\gamma}_{SE}$  with  $N_S = N_R = N_E = 2$ ,  $\alpha = 2.296$ ,  $\beta = 2$ ,  $\xi = 6.7$ ,  $r = 2$ ,  $\rho_{RF} = \rho_{FSO} = 0.7$ ,  $m = 2$ ,  $\bar{\gamma}_{SD} = 5$  dB, and  $R_s = 0.1$ .

Then we can express the SOP with OTAS scheme as

$$\begin{aligned}
 P_{out}^{OTAS} &= \Pr \{ C_{s,b_{OTAS}}^{OTAS} \leq R_s \} \\
 &= \Pr \{ \max (C_{s,i}^{OTAS}) \leq R_s \} \\
 &= \Pr \{ C_{s,i}^{OTAS} \leq R_s, \dots, C_{s,N_S}^{OTAS} \leq R_s \}.
 \end{aligned} \tag{27}$$

However, it is challenging to obtain the closed-form solutions for SOP under OTAS because  $C_{s,i}^{OTAS}$  are not independent of each other. Another important reason is that it is very difficult to obtain the exact CSI of  $R$ - $D$  for  $S$  due to estimation errors and delays. In Section IV, simulation results of SOP under OTAS are given as a benchmark with the assumption that  $S$  has the imperfect CSI of FSO link without delay.

In the following, three different suboptimal TAS schemes are proposed to enhance the secrecy performance of the mixed RF-FSO systems.

### B. SOP with TAS based on $S$ - $R$ link

Substituting (11) and (13) into (25), then utilizing (3.326.2) of [40], (8) of [44], and (21) of [45], we obtain

$$\begin{aligned}
 P_{out,1}^L &= \int_0^\infty F_{\gamma_{eq,1}}(\Theta\gamma) f_{\gamma_{SE,1}}(\gamma) d\gamma \\
 &= 1 - \phi_R \sum_{S_R} \sum_{q=0}^{B_R} \sum_{t=0}^{q+\tau_R-1} \Xi \left( Z_0(t + \tau_E - 1)! - B_D \sum_{h=1}^{\beta} \sum_{k=0}^{\infty} \phi_2 G_{r+2,2r}^{r,r+2} [v_1 |_{K_2}^{K_1}] \right),
 \end{aligned} \tag{28}$$

where  $\Xi = \frac{\varphi_R \Theta^t \lambda_E^{\tau_E}}{\Gamma(\tau_E) \phi_1^{t+\tau_E}}$ ,  $\phi_1 = v_R \Theta + \lambda_E$ ,  $\phi_2 = H_1 r^{\frac{k}{2}} 2^{t+\tau_E-0.5} / (2\pi)^{0.5r}$ ,  $K_1 = [\Delta(r, 1), \Delta(2, 1 - t - \tau_E)]$ ,  $K_2 = [\Delta(r, \frac{1+k}{2}), \Delta(r, 0)]$ ,  $\Delta(k, a) = [\frac{a}{k}, \frac{a+1}{k}, \dots, \frac{a+k-1}{k}]$ , and  $v_1 = \frac{4\psi_1^r \Theta^2}{r^r \phi_1^2}$ .

Using the Meijer's  $G$ -function expansion given in [46], we obtain the asymptotic SOP when  $\bar{\gamma}_{RD} \rightarrow \infty$  as

$$P_{out,1}^{L,\infty} = 1 + \phi_R \sum_{S_R} \sum_{q=0}^{B_R} \sum_{t=0}^{q+\tau_R-1} \Xi \left( B_D \sum_{h=1}^{\beta} \sum_{k=0}^{\infty} \phi_2 \Phi_1 - Z_0(t + \tau_E - 1)! \right), \quad (29)$$

$$\text{where } \Phi_1 = \sum_{l=1}^r \frac{\prod_{j=1, j \neq l}^r \Gamma(K_{2,j} - K_{2,l}) \prod_{j=1}^{r+2} \Gamma(1 + K_{2,l} - K_{1,j})}{v_1^{-K_{2,l}} \prod_{j=r+1}^{2r} \Gamma(1 + K_{2,l} - K_{2,j})}.$$

### C. SOP with TAS based on S-E link

Substituting (18) and (23) into (25) and after some algebraic manipulations, we obtain

$$\begin{aligned} P_{out,2}^L &= \int_0^{\infty} F_{\gamma_{eq,2}}(\Theta\gamma) f_{\hat{\gamma}_{SE,2}}(\gamma) d\gamma \\ &= 1 - \phi_E \sum_{S_E} \sum_{q=0}^{B_E} \sum_{i=0}^{\tau_R-1} \Lambda_E \Psi \left( Z_0(i + q + \tau_E - 1)! - B_D \sum_{h=1}^{\beta} \sum_{k=0}^{\infty} \phi_4 G_{r+2,2r}^{r,r+2} [v_2 \left| \frac{K_3}{K_2} \right] \right), \end{aligned} \quad (30)$$

where  $\Psi = \frac{(\Theta \lambda_R)^i}{\phi_3^{i+q+\tau_E} i!}$ ,  $v_2 = \frac{4\psi_1^r \Theta^2}{r^r \phi_3^2}$ ,  $\phi_3 = \Theta \lambda_R + v_E$ ,  $\phi_4 = \frac{H_1 r^{\frac{k}{2}} 2^{i+q+\tau_E-0.5}}{(2\pi)^{0.5r}}$ , and  $K_3 = [\Delta(r, 1), \Delta(2, 1 - i - q - \tau_E)]$ .

Similar to (29), we obtain the asymptotic SOP for this scenario as

$$P_{out,2}^{L,\infty} = 1 + \phi_E \sum_{S_E} \sum_{q=0}^{B_E} \sum_{i=0}^{\tau_R-1} \Lambda_E \Psi \left( B_D \sum_{h=1}^{\beta} \sum_{k=0}^{\infty} \phi_4 \Phi_2 - Z_0(i + q + \tau_E - 1)! \right), \quad (31)$$

$$\text{where } \Phi_2 = \sum_{l=1}^r \frac{\prod_{j=1, j \neq l}^r \Gamma(K_{2,j} - K_{2,l}) \prod_{j=1}^{r+2} \Gamma(1 + K_{2,l} - K_{3,j})}{v_2^{-K_{2,l}} \prod_{j=r+1}^{2r} \Gamma(1 + K_{2,l} - K_{2,j})}.$$

### D. A new adaptive TAS Scheme

In this part, an adaptive TAS scheme is proposed to improve the secrecy performance for the considered system. To obtain a LOS transmission,  $R$  (the sender of FSO link) must be located at some place with high altitude, such as the building roof. In other words, the location of  $R$

is limited while designing a mixed RF-FSO system. Thus we propose an adaptive TAS scheme, the criterion of which is expressed as

$$b_3 = \begin{cases} b_2, & \text{when } \bar{\gamma}_{SR} > \bar{\gamma}_{RD} \\ b_2, & \text{when } (\bar{\gamma}_{SR} < \bar{\gamma}_{RD}) \cup (\bar{\gamma}_{SR} < \bar{\gamma}_{SE}) \\ b_1, & \text{when } (\bar{\gamma}_{SR} < \bar{\gamma}_{RD}) \cup (\bar{\gamma}_{SR} > \bar{\gamma}_{SE}) \end{cases} . \quad (32)$$

The adaptive scheme is explained as follows. When the relay is located in those places that makes  $\bar{\gamma}_{SR} > \bar{\gamma}_{RD}$ ,  $R$ - $D$  link becomes the bottleneck of the equivalent SNR at  $D$ . Under this scenario, the secrecy performance of the considered system depends on  $S$ - $E$  and  $R$ - $D$  links. Thus, we select antenna based on  $S$ - $E$  link (defined by (15)) where the CSI of  $E$  is known at  $S$ . On the other hand, when  $R$  is located on those places that makes  $\bar{\gamma}_{SR} < \bar{\gamma}_{RD}$ ,  $S$ - $R$  link becomes bottleneck of the equivalent SNR at  $D$ . Under such a scenario, the secrecy performance of the considered system depends on the first hop. Thus, we select antenna based on  $S$ - $R$  link (defined by (5)) when  $S$  does not has the CSI of  $E$ . Moreover, when  $S$  has the CSI of  $E$  and  $\bar{\gamma}_{SR} < \bar{\gamma}_{RD}$ , we select the antenna based on the CSI of  $S$ - $E$  links when  $\bar{\gamma}_{SR} < \bar{\gamma}_{SE}$ . Otherwise, we select the antenna based on the CSI of  $S$ - $R$  links when  $\bar{\gamma}_{SR} > \bar{\gamma}_{SE}$ .

Obviously, one can find that the adaptive TAS scheme just based on the average SNR of RF links and FSO link, which are always easy to obtain. But the results is rough and not always the best when the different between the RF link and FSO link is small (see Fig. 4). If the source can calculate the SOP, the adaptive TAS scheme can be represented as

$$b_3 = \arg \min_{i=1,2} P_{out,i}. \quad (33)$$

*Remark 5:* Since we are considering only part of the system and not the complete system, the secrecy performance with TAS scheme based on  $S$ - $R$  links or  $S$ - $E$  links will not exceed that with OTAS.

#### IV. NUMERICAL RESULTS AND DISCUSSIONS

In this part, we present some representative Monte-Carlo simulation results to explain the behavior of SOP with respect to different TAS schemes and the parameters of the considered system. The main parameters utilized are set as  $I_l = 1$ ,  $A_0 = 1$ ,  $\Omega = 1.32$ ,  $b_0 = 0.1097$ ,  $\rho_0 = 0.6$ ,  $\varphi_A - \varphi_B = \frac{\pi}{2}$ ,  $\rho_{SR} = \rho_{SE} = \rho_{RF}$ ,  $m_R = m_E = m$ , and  $R_s = 0.01$  bit/s/Hz. In all the figures, ‘TASR’ and ‘TASE’ signify the TAS scheme based on  $S$ - $R$  or  $S$ - $E$  links, respectively. The

simulation/numerical results with adaptive TAS scheme are omitted since one can easily obtain them based on those with TASR and TASE schemes.

Figs. 4 - 8 show the SOP with different TAS schemes for various  $\bar{\gamma}_{SE}$ ,  $r$ ,  $\xi$ , and  $(\alpha, \beta)$ , respectively. One can observe that the simulation results match the numerical results very well. The SOP decreases significantly with increasing  $\bar{\gamma}_{RD}$  and there is a floor since the equivalent SNRs at  $D$  will be equal to the SNR of  $S-R$  link. Furthermore, one can observe that the SOP with TASE is equal to that of OTAS, and is better than that of TASR in lower- $\bar{\gamma}_{RD}$  region. This is because that the SOP is independent of  $S-R$  link in these areas and OTAS equals to TASE. In the higher- $\bar{\gamma}_{RD}$  region, TASR scheme can obtain better secrecy performance compared with TASE scheme when  $\bar{\gamma}_{SR} > \bar{\gamma}_{SE}$ , which can be found from Fig. 4. Vice versa, in those scenarios when  $\bar{\gamma}_{SR} < \bar{\gamma}_{SE}$ , the SOP of TASE outperforms that of TASR since  $S-E$  link is the major factor.

From Figs. 5, 6, and 7, it can be observed that the SOP with  $r = 1$  or  $\xi = 6.7$  or  $(\alpha = 4.3, \beta = 3)$  outperforms that with  $r = 2$  or  $\xi = 1.1$  or  $(\alpha = 1.53, \beta = 1)$  since smaller SNR can be obtained for  $R-D$  link in the former cases relative to the latter ones. These latter scenarios signify IM/DD detect technology, larger pointing error, and stronger atmospheric turbulence conditions, respectively. Figs. 8 and 9 demonstrate that the SOP with larger correlation coefficients outperform the ones with smaller correlation coefficient because the smaller correlation coefficients signify severely outdated effect (for RF links) or larger channel estimation errors (for FSO links).

Figs. 10 - 13 demonstrate the SOP with different TAS schemes for various  $N_S$ ,  $N_R$ ,  $N_E$ , and  $m$ , respectively. One can draw conclusion from Fig. 10 that increasing  $N_S$  is not an effective method to enhance the secrecy performance of the considered system. As observed from Figs. 11 and 12, we can observe that the effect of the number of eavesdroppers on the SOP is greater than that of the number of antennas at  $R$ , especially for the SOP with TASE and OTAS. From Fig. 13, we can deduce that in the lower- $\bar{\gamma}_{SR}$  region, the SOP with smaller  $m$  is better than that with larger  $m$ , which is consistent with the results in [47]. In this region,  $S-R$  link is the bottleneck for the equivalent SNR at  $D$  and the system behaves synonymous to a MIMO RF Wyner model, which was considered with perfect CSI in [47].

Furthermore, relative to the results in [30], one can observe that the secrecy performance of the considered system deteriorates due to imperfect CSI, which is consistent with the results in [33].



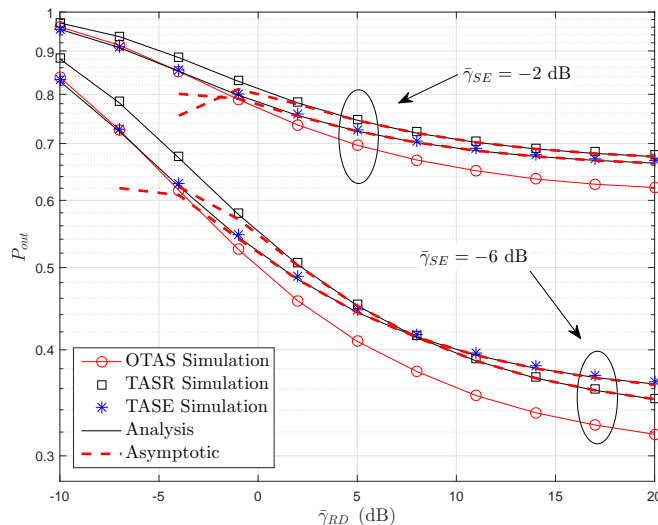


Fig. 4. SOP for various  $\bar{\gamma}_{SE}$  with  $N_S = 5$ ,  $N_R = N_E = 2$ ,  $\alpha = 2.296$ ,  $\beta = 2$ ,  $\xi = 6.7$ ,  $r = 2$ ,  $\rho_{RF} = 0.7$ ,  $\rho_{FSO} = 0.5$ ,  $m = 2$ , and  $\bar{\gamma}_{SR} = -4$  dB.

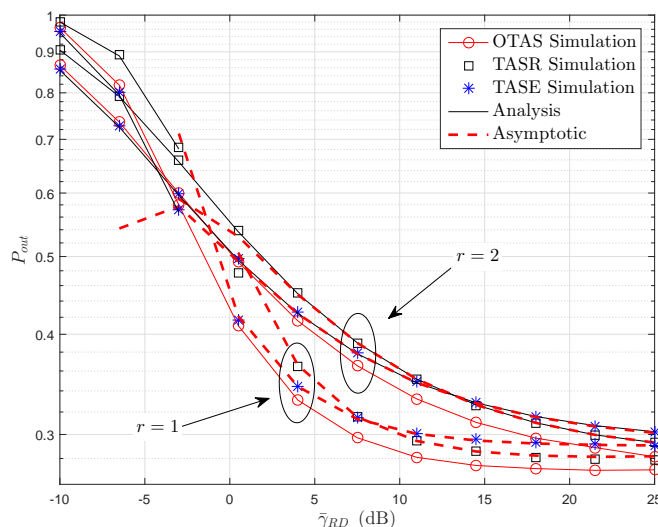


Fig. 5. SOP for various  $r$  with  $N_S = 5$ ,  $N_R = N_E = 2$ ,  $\alpha = 2.296$ ,  $\beta = 2$ ,  $\xi = 6.7$ ,  $\rho_{RF} = 0.7$ ,  $\rho_{FSO} = 0.5$ ,  $m = 2$ ,  $\bar{\gamma}_{SR} = -1$  dB, and  $\bar{\gamma}_{SE} = -5$  dB.

## V. CONCLUSION

Three different TAS schemes were proposed to improve the secrecy performance of mixed RF-FSO systems while imperfect CSI was considered. We analyzed the secrecy outage performance with different TAS schemes and the closed-form expressions for the lower bound and asymptotic SOP with different TAS were obtained. The effect of TAS schemes and parameters of mixed RF-FSO systems on the SOP were investigated. The results demonstrated that the proposed

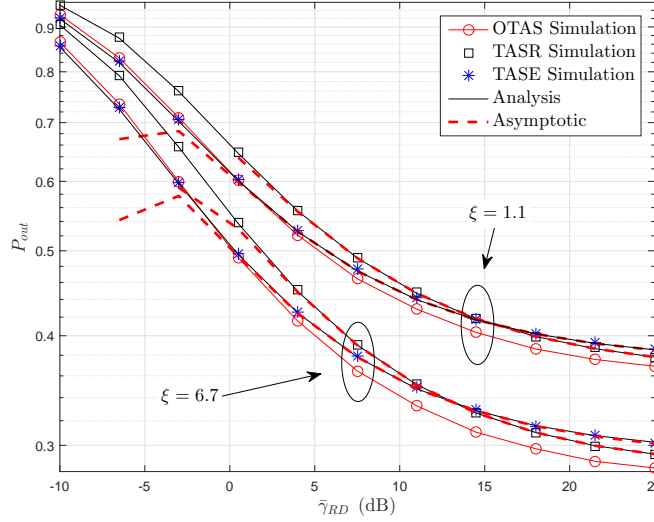


Fig. 6. SOP for various  $\xi$  with  $N_S = 5$ ,  $N_R = N_E = 2$ ,  $\alpha = 2.296$ ,  $\beta = 2$ ,  $\rho_{RF} = 0.7$ ,  $\rho_{FSO} = 0.5$ ,  $m = 2$ ,  $\tilde{\gamma}_{SR} = -1$  dB, and  $\tilde{\gamma}_{SE} = -5$  dB.

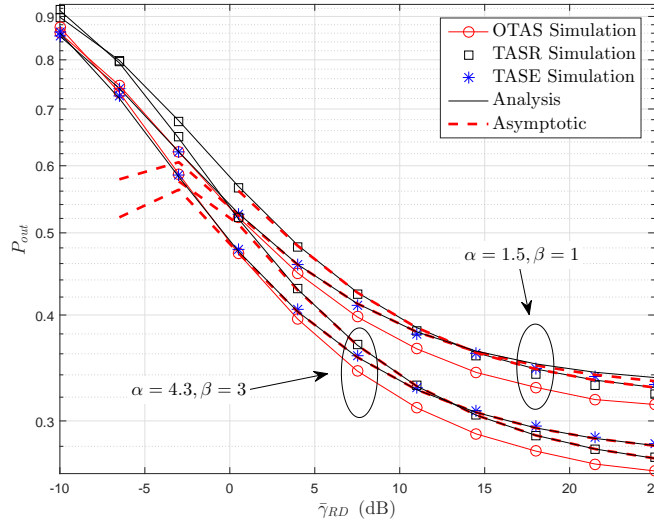


Fig. 7. SOP for various  $\alpha, \beta$  with  $N_S = 5$ ,  $N_R = N_E = 2$ ,  $\xi = 6.7$ ,  $r = 2$ ,  $\rho_{RF} = 0.7$ ,  $\rho_{FSO} = 0.5$ ,  $m = 2$ ,  $\tilde{\gamma}_{SR} = -1$  dB, and  $\tilde{\gamma}_{SE} = -5$  dB.

TAS schemes can enhance the secrecy performance. Meanwhile, comparing our results with the results in [30], [31], [33], one can observe that the imperfect/outdated CSI seriously deteriorates the secrecy performance of mixed RF-FSO systems. Hereafter, more attention must be given to enhance the secrecy performance of mixed RF-FSO systems with imprecise CSI.

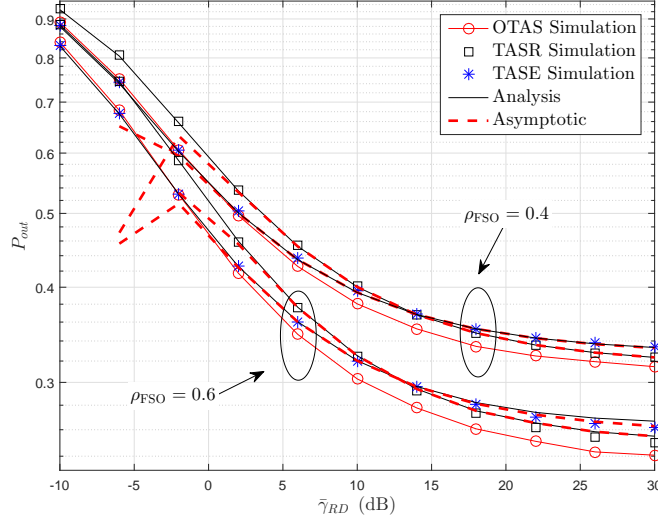


Fig. 8. SOP for various  $\rho_{\text{FSO}}$  with  $N_S = 5$ ,  $N_R = N_E = 2$ ,  $\alpha = 2.296$ ,  $\beta = 2$ ,  $\xi = 6.7$ ,  $r = 2$ ,  $\rho_{\text{RF}} = 0.7$ ,  $m = 2$ ,  $\bar{\gamma}_{\text{SR}} = -1$  dB, and  $\bar{\gamma}_{\text{SE}} = -5$  dB.

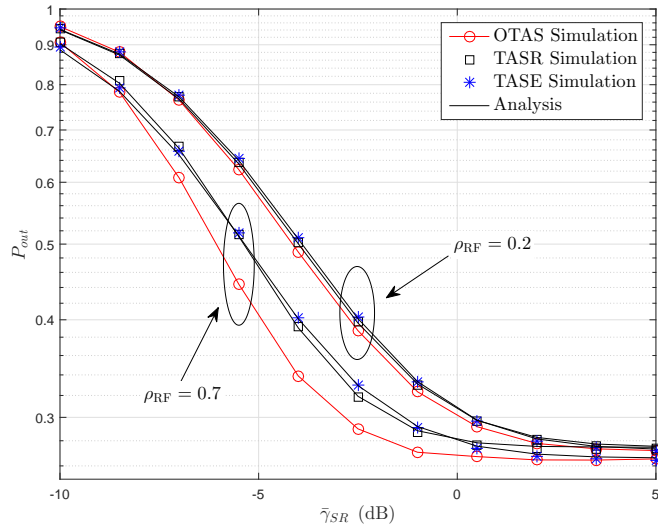


Fig. 9. SOP for various  $\rho_{\text{RF}}$  with  $N_S = 5$ ,  $N_R = N_E = 2$ ,  $\alpha = 2.296$ ,  $\beta = 2$ ,  $r = 2$ ,  $\xi = 6.7$ ,  $m = 2$ ,  $\rho_{\text{FSO}} = 0.5$ ,  $\bar{\gamma}_{\text{RD}} = 15$  dB, and  $\bar{\gamma}_{\text{SE}} = -5$  dB.

## APPENDIX A

The PDF of  $h_{\text{RD}}$  is given as [35]

$$f_{h_{\text{RD}}}(x) = \frac{\xi^2 A_D}{2x} \sum_{h=1}^{\beta} b_h G_{1,3}^{3,0} \left[ \delta_0 x \left| \begin{matrix} \xi^2 + 1 \\ \xi^2, \alpha, h \end{matrix} \right. \right], \quad (34)$$

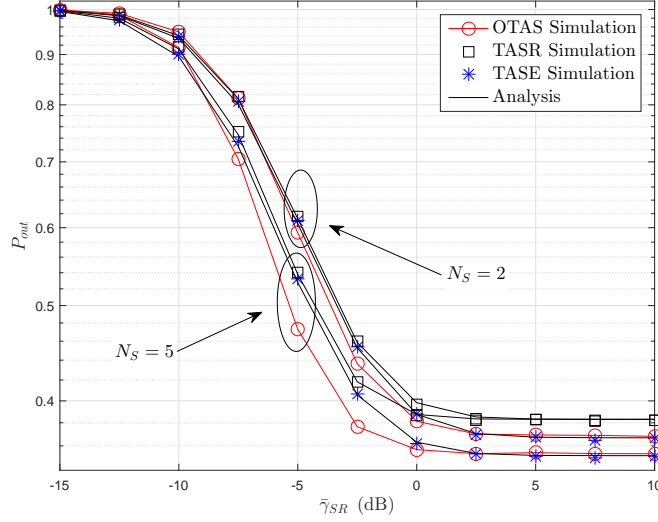


Fig. 10. SOP for various  $N_S$  with  $N_R = 2$ ,  $N_E = 2$ ,  $\alpha = 2.296$ ,  $\beta = 2$ ,  $\xi = 6.7$ ,  $r = 2$ ,  $\rho_{RF} = 0.7$ ,  $\rho_{FSO} = 0.6$ ,  $m = 2$ ,  $\tilde{\gamma}_{RD} = 5$  dB, and  $\tilde{\gamma}_{SE} = -5$  dB.

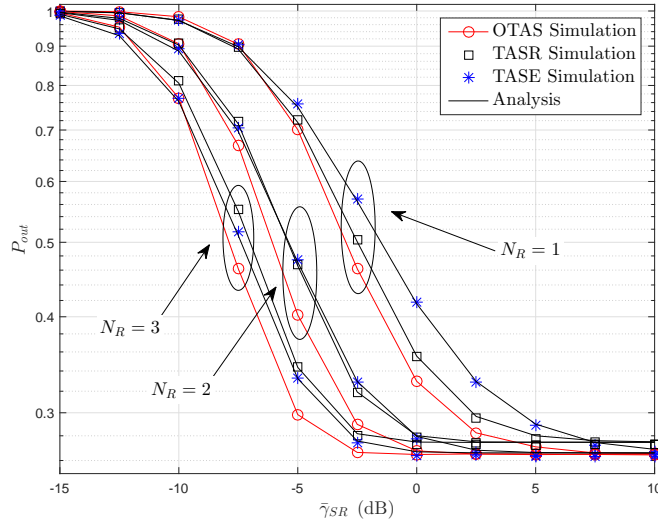


Fig. 11. SOP for various  $N_R$  with  $N_S = 5$ ,  $N_E = 2$ ,  $\alpha = 2.296$ ,  $\beta = 2$ ,  $\xi = 6.7$ ,  $r = 2$ ,  $\rho_{RF} = 0.7$ ,  $\rho_{FSO} = 0.6$ ,  $m = 2$ ,  $\tilde{\gamma}_{RD} = 15$  dB, and  $\tilde{\gamma}_{SE} = -5$  dB.

where  $A_D = \frac{2\alpha^{0.5\alpha}}{g^{1+0.5\alpha}\Gamma(\alpha)} \left(\frac{g\beta}{g\beta+\Omega_1}\right)^{\beta+0.5\alpha}$ ,  $b_h = \frac{(\beta-1)!(g\beta+\Omega_1)^{1-0.5h}\alpha^{0.5h}\Omega_1^{h-1}}{((h-1)!)^2(\beta-h)!\beta^{0.5h}g^{h-1}} \left(\frac{\alpha\beta}{g\beta+\Omega_1}\right)^{-0.5(\alpha+h)}$ , and  $\delta_0 = \frac{\alpha\beta}{(g\beta+\Omega_1)I_l A_0}$ .

Let  $X = \rho_{FSO}h_{RD}$ ,  $Y = \sqrt{1 - \rho_{FSO}^2}\varepsilon$ , and  $Z = \hat{h}_{RD}$ , one can easily obtain

$$f_X(z) = \frac{\xi^2 A_D}{2z} \sum_{h=1}^{\beta} b_h G_{1,3}^{3,0} \left[ \delta z \left| \begin{matrix} \xi^2+1 \\ \xi^2, \alpha, h \end{matrix} \right. \right], \quad (35)$$

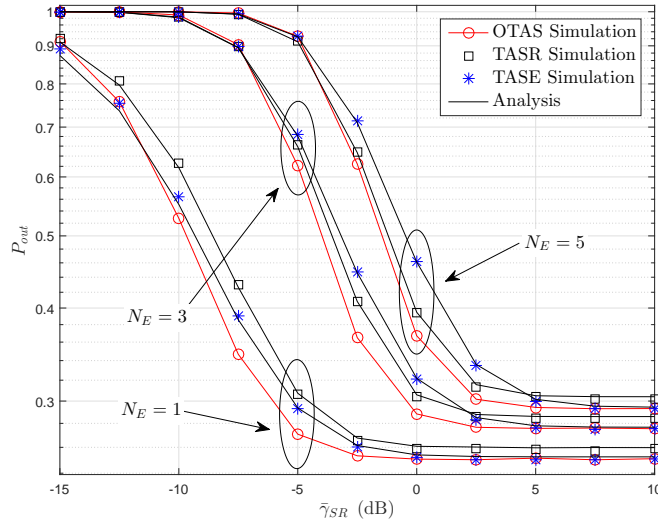


Fig. 12. SOP for various  $N_E$  with  $N_S = 5$ ,  $N_R = 2$ ,  $\alpha = 2.296$ ,  $\beta = 2$ ,  $\xi = 6.7$ ,  $r = 2$ ,  $\rho_{RF} = 0.7$ ,  $\rho_{FSO} = 0.6$ ,  $m = 2$ ,  $\bar{\gamma}_{RD} = 15$  dB, and  $\bar{\gamma}_{SE} = -5$  dB.

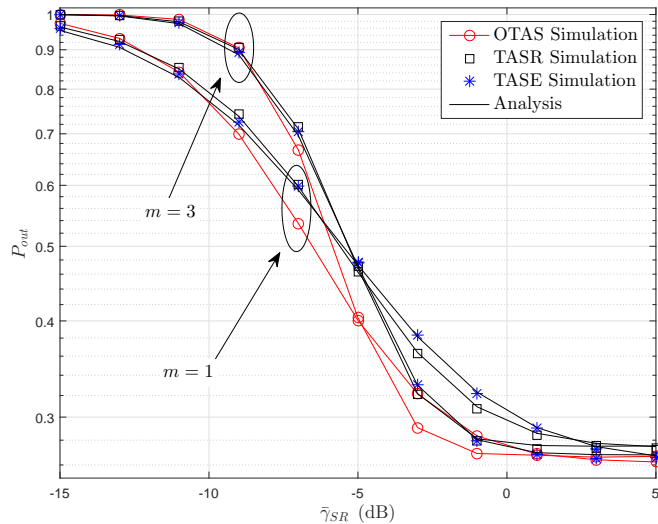


Fig. 13. SOP for various  $m$ ,  $N_S = 5$ ,  $N_R = N_E = 2$ ,  $r = 2$ ,  $\alpha = 2.296$ ,  $\beta = 2$ ,  $r = 2$ ,  $\xi = 6.7$ ,  $\rho_{FSO} = 0.6$ ,  $\bar{\gamma}_{RD} = 15$  dB, and  $\bar{\gamma}_{SE} = -5$  dB.

$$f_Y(y) = \frac{1}{\sqrt{2\pi(1-\rho_{FSO}^2)}} e^{-\frac{y^2}{2(1-\rho_{FSO}^2)}}, \quad (36)$$

where  $\delta = \frac{\alpha\beta}{(g\beta + \Omega_1)I_l A_0 \rho_{FSO}}$ .

According to the convolution theorem, the PDF of  $Z$  can be obtained as

$$\begin{aligned} f_Z(z) &= \int_0^\infty f_X(x) f_Y(z-x) dx \\ &= \frac{\xi^2 A_D}{2\sqrt{2\pi}(1-\rho_{\text{FSO}}^2)} \sum_{h=1}^{\beta} b_h e^{-\frac{z^2}{2(1-\rho_{\text{FSO}}^2)}} \nabla, \end{aligned} \quad (37)$$

where

$$\nabla = \int_0^\infty \frac{1}{x} e^{\frac{zx}{1-\rho_{\text{FSO}}^2}} e^{-\frac{x^2}{2(1-\rho_{\text{FSO}}^2)}} G_{1,3}^{3,0} \left[ \delta x \left| \begin{matrix} \xi^2+1 \\ \xi^2, \alpha, h \end{matrix} \right. \right] dx.$$

Using (11) and (21) of [45], (9.31.5) of [40], and  $e^x = \sum_{k=0}^{\infty} \frac{x^k}{k!}$ , we obtain

$$\nabla = \frac{2^{\alpha-3}}{\pi} \sum_{k=0}^{\infty} \frac{2^{0.5k+h} G_k}{k!(1-\rho_{\text{FSO}}^2)^{\frac{k}{2}}} z^k, \quad (38)$$

where  $G_k = G_{6,3}^{1,6} \left[ \frac{2^3}{\delta^2(1-\rho_{\text{FSO}}^2)} \left| \begin{matrix} \frac{1-\xi^2}{2}, \frac{2-\xi^2}{2}, \frac{1-\alpha}{2}, \frac{2-\alpha}{2}, \frac{1-h}{2}, \frac{2-h}{2} \\ k, \frac{-\xi^2}{2}, \frac{1-\xi^2}{2} \end{matrix} \right. \right]$ .

Substituting (38) into (37), we obtain

$$f_Z(z) = B_D \sum_{h=1}^{\beta} \sum_{k=0}^{\infty} H_0 e^{-\frac{z^2}{2(1-\rho_{\text{FSO}}^2)}} z^k, \quad (39)$$

where  $B_D = \frac{\xi^2 A_D 2^{\alpha-4.5}}{\pi^{1.5}}$  and  $H_0 = \frac{2^{0.5k+h} b_h G_k}{k!(1-\rho_{\text{FSO}}^2)^{\frac{k+1}{2}}}$ .

It must be noted that the channel gain of FSO link is positive in practical models [32]. Thus, we rewrite  $f_{\hat{h}_D}(x)$  as

$$f_{\hat{h}_{RD}}(x) = \begin{cases} B_D \sum_{h=1}^{\beta} \sum_{k=0}^{\infty} H_0 e^{-\frac{x^2}{2(1-\rho_{\text{FSO}}^2)}} x^k, & x > 0 \\ 1 - Z_0, & x = 0 \end{cases}, \quad (40)$$

where  $Z_0$  is obtained by  $\int_0^\infty f_{\hat{h}_{RD}}(x) dx = 1$ . Utilizing (3.326.2) of [40], we obtain

$$\begin{aligned} Z_0 &= B_D \sum_{h=1}^{\beta} \sum_{k=0}^{\infty} H_0 \int_0^\infty x^k e^{-\frac{x^2}{2(1-\rho_{\text{FSO}}^2)}} dx \\ &= \frac{\xi^2 A_D}{\pi^{1.5}} \sum_{h=1}^{\beta} \sum_{k=0}^{\infty} \frac{2^{k+\alpha+h-5} b_h G_k}{k!} \Gamma\left(\frac{k+1}{2}\right). \end{aligned} \quad (41)$$

Utilizing (07.34.21.0084.01) in [48], we obtain the CDF of  $\hat{h}_{RD}$  as

$$F_{\hat{h}_D}(x) = \begin{cases} B_D \sum_{h=1}^{\beta} \sum_{k=0}^{\infty} H_1 G_{1,2}^{1,1} \left[ \frac{x^2}{2(1-\rho_{\text{FSO}}^2)} \middle| \frac{1}{\frac{k+1}{2}, 0} \right], & x > 0 \\ 1 - Z_0, & x = 0 \end{cases}, \quad (42)$$

where  $H_1 = \frac{b_h 2^{k+h-0.5} G_k}{k!}$ .

Although the expression of the CDF in (42) includes the infinite summation, the truncation errors with the similar method given in [33] proved that the infinite summation is convergent with a finite truncation.

Based on (2), we obtain the result in (3) and (4).

## APPENDIX B

The PDF and CDF of  $\gamma_{S_iR} = \frac{P_S}{N_0} \sum_{j=1}^{N_R} |h_{S_iR_j}|^2$  are given by [36]

$$f_{\gamma_{S_iR}}(x) = \frac{\lambda_R^{\tau_R}}{\Gamma(\tau_R)} e^{-\lambda_R x} x^{\tau_R-1}, \quad (43)$$

$$F_{\gamma_{S_iR}}(x) = 1 - \sum_{i=0}^{\tau_R-1} \frac{e^{-\lambda_R x}}{i!} (\lambda_R x)^i, \quad (44)$$

respectively, where  $\lambda_R = \frac{m_R}{\bar{\gamma}_R}$ ,  $\tau_R = m_R N_R$ , and  $\bar{\gamma}_R$  is the average SNR of  $S - R$  link.

The PDF of  $\hat{\gamma}_{SR}$  can be obtained by [11]

$$\begin{aligned} f_{\hat{\gamma}_{SR}}(x) &= \int_0^{\infty} f_{\hat{\gamma}_{SR}|\gamma_{SR}}(x|y) f_{\gamma_{SR,1}}(y) dy \\ &= \int_0^{\infty} \frac{f_{\hat{\gamma}_{S_iR}, \gamma_{S_iR}}(x, y)}{f_{\gamma_{S_iR}}(y)} f_{\gamma_{SR,1}}(y) dy, \end{aligned} \quad (45)$$

where  $\gamma_{SR,1} = \max_{1 \leq i \leq N_S} \{\gamma_{S_iR}\}$  and the joint PDF  $f_{\hat{\gamma}_{S_iR}, \gamma_{S_iR}}(x, y)$  is given by [49]

$$\begin{aligned} f_{\hat{\gamma}_{S_iR}, \gamma_{S_iR}}(x, y) &= \frac{\lambda_R^{\tau_R+1}}{(1-\rho_{SR}^2) \Gamma(\tau_R)} \left( \frac{xy}{\rho_{SR}^2} \right)^{\frac{\tau_R-1}{2}} \\ &\times e^{-\frac{(x+y)\lambda_R}{1-\rho_{SR}^2}} I_{\tau_R-1} \left( \frac{2\lambda_R \rho_{SR} \sqrt{xy}}{1-\rho_{SR}^2} \right), \end{aligned} \quad (46)$$

where  $I_n(x)$  is the  $n$ -th order modified Bessel function of first kind, defined as (8.406.1) of [40].

Based on  $\gamma_{SR,1} = \max_{1 \leq i \leq N_S} \{\gamma_{S_i R}\}$ , and using (44) and multinomial theorem [39], we obtain the PDF of  $\gamma_{SR,1}$  as

$$\begin{aligned} f_{\gamma_{SR,1}}(x) &= N_S \left( F_{\gamma_{S_i R}}(x) \right)^{N_S-1} f_{\gamma_{S_i R}}(x) \\ &= \frac{N_S \lambda_R^{\tau_R}}{\Gamma(\tau_R)} \sum_{S_R} A_R x^{B_R + \tau_R - 1} e^{-\lambda_R (C_R + 1)x}, \end{aligned} \quad (47)$$

where  $S_R = \left\{ (n_1, \dots, n_{\tau_R+1}) \in \mathbb{N} \left| \sum_{p=1}^{\tau_R+1} n_p = N_S - 1 \right. \right\}$ ,  $A_R = \left( \frac{N_S - 1}{\prod_{q=1}^{\tau_R+1} n_q} \right)^{\tau_R+1} \prod_{p=2}^{\tau_R+1} \left( -\frac{\lambda_R^{p-2}}{(p-2)!} \right)^{n_p}$ ,

$B_R = \sum_{p=2}^{\tau_R+1} n_p (p-2)$ ,  $C_R = \sum_{p=2}^{\tau_R+1} n_p$ , and  $\mathbb{N}$  denotes a non-negative integer set.

Substituting (46) and (47) into (45), we have

$$\begin{aligned} f_{\hat{\gamma}_{SR}}(x) &= \frac{N_S \lambda_R^{\tau_R+1}}{(1 - \rho_{SR}^2) \Gamma(\tau_R)} \left( \frac{x}{\rho_{SR}^2} \right)^{\frac{\tau_R-1}{2}} \sum_{S_R} A_R e^{-\frac{\lambda_R x}{1 - \rho_{SR}^2}} \\ &\quad \times \int_0^\infty y^{B_R + \frac{\tau_R-1}{2}} e^{-\chi_1 y} I_{\tau_R-1}(2\chi_2 \sqrt{xy}) dy, \end{aligned} \quad (48)$$

where  $\chi_1 = \lambda_R \left( \frac{1}{1 - \rho_{SR}^2} + C_R \right)$  and  $\chi_2 = \frac{\lambda_R \rho_{SR}}{1 - \rho_{SR}^2}$ .

Making use of (8.406.3), (6.643.4), and (8.970.1) of [40], and after some algebraic manipulations, we obtain (8) and (9), respectively.

### APPENDIX C

The PDF and CDF of  $\gamma_{S_i E} = \frac{P_S}{N_0} \sum_{j=1}^{N_E} |h_{S_i E_j}|^2$  are given by [36]

$$f_{\gamma_{S_i E}}(x) = \frac{\lambda_E^{\tau_E}}{\Gamma(\tau_E)} e^{-\lambda_E x} x^{\tau_E-1}, \quad (49)$$

$$F_{\gamma_{S_i E}}(x) = 1 - \sum_{i=0}^{\tau_E-1} \frac{e^{-\lambda_E x}}{i!} (\lambda_E x)^i, \quad (50)$$

respectively, where  $\lambda_E = \frac{m_E}{\bar{\gamma}_E}$ ,  $\tau_E = m_E N_E$ , and  $\bar{\gamma}_E$  is the average SNR of  $S$ - $E$  link.

The PDF of  $\hat{\gamma}_{SE}$  can be obtained by [11]

$$\begin{aligned} f_{\hat{\gamma}_{SE}}(x) &= \int_0^\infty f_{\hat{\gamma}_{SE}|\gamma_{SE}}(x|y) f_{\gamma_{SE,2}}(y) dy \\ &= \int_0^\infty \frac{f_{\hat{\gamma}_{S_i E}, \gamma_{S_i E}}(x, y)}{f_{\gamma_{S_i E}}(y)} f_{\gamma_{SE,2}}(y) dy, \end{aligned} \quad (51)$$



where  $\gamma_{SE,2} = \min_{1 \leq i \leq N_S} \{\gamma_{S_i E}\}$  and the joint PDF  $f_{\hat{\gamma}_{S_i E}, \gamma_{S_i E}}(x, y)$  is given by [49]

$$f_{\hat{\gamma}_{S_i E}, \gamma_{S_i E}}(x, y) = \frac{\lambda_E^{\tau_E+1}}{(1 - \rho_{SE}^2) \Gamma(\tau_E)} \left( \frac{xy}{\rho_{SE}^2} \right)^{\frac{\tau_E-1}{2}} \times e^{-\frac{(x+y)\lambda_E}{1-\rho_{SE}^2}} I_{\tau_E-1} \left( \frac{2\lambda_E \rho_{SE} \sqrt{xy}}{1 - \rho_{SE}^2} \right). \quad (52)$$

Making using of multinomial theorem, we obtain the PDF of  $\gamma_{SE,2}$  as

$$f_{\gamma_{SE,2}}(x) = N_S \left(1 - F_{\gamma_{S_i E}}(x)\right)^{N_S-1} f_{\gamma_{S_i E}}(x) = \frac{N_S \lambda_E^{\tau_E}}{\Gamma(\tau_E)} \sum_{S_E} A_E x^{B_E + \tau_E - 1} e^{-\lambda_E (C_E + 1)x}, \quad (53)$$

where  $S_E = \left\{ (n_1, \dots, n_{\tau_E}) \in \mathbb{Z}^{\geq} \left| \sum_{p=1}^{\tau_E} n_p = N_S - 1 \right. \right\}$ ,  $A_E = \left( \frac{N_S - 1}{\tau_E} \prod_{q=1}^{\tau_E} n_q \right) \prod_{p=1}^{\tau_E} \left( \frac{\lambda_E^{p-1}}{(p-1)!} \right)^{n_p}$ ,  $B_E = \sum_{p=1}^{\tau_E} n_p (p-1)$ , and  $C_E = \sum_{p=1}^{\tau_E} n_p$ .

Substituting (46) and (53) into (45), we have

$$f_{\hat{\gamma}_{SE}}(x) = \frac{N_S \lambda_E^{\tau_E+1}}{(1 - \rho_{SE}^2) \Gamma(\tau_E)} \left( \frac{x}{\rho_{SE}^2} \right)^{\frac{\tau_E-1}{2}} \sum_{S_E} A_E e^{-\frac{\lambda_E x}{1-\rho_{SE}^2}} \times \int_0^\infty y^{B_E + \frac{\tau_E-1}{2}} e^{-\chi_3 y} I_{\tau_E-1} (2\chi_4 \sqrt{xy}) dy, \quad (54)$$

where  $\chi_3 = \lambda_R \left( \frac{1}{1-\rho_{SE}^2} + C_E \right)$  and  $\chi_4 = \frac{\lambda_E \rho_{SE}}{1-\rho_{SE}^2}$ .

Making use of (8.406.3), (6.643.4), and (8.970.1) of [40], and after some algebraic manipulations, we obtain (18) and (19), respectively.

## REFERENCES

- [1] Y. Li, J. Liu, B. Cao, and C. Wang, "Joint Optimization of radio and virtual machine resources with uncertain user demands in mobile cloud computing," *IEEE Trans. on Multimedia*, vol. 20, no. 9, pp. 2427 - 2438, Sept. 2018.
- [2] D. Kedar and S. Arnon, "Urban optical wireless communication networks: The main challenges and possible solutions," *IEEE Commun. Mag.*, vol. 42, no. 5, pp. S2-S7, May 2004.
- [3] Z. Zhang, T. Zeng, X. Yu, and S. Sun, "Social-aware D2D pairing for cooperative video transmission using matching theory," *Mobile Netw. Appl.*, vol. 23, no. 3, pp. 639-649, Jun. 2018.
- [4] Z. Zhang, P. Zhang, D. Liu, and S. Sun, "SRSM-based adaptive relay selection for D2D communications," *IEEE Internet of Things Journal*, vol. 5, no. 4, pp. 232-2332, Aug. 2018.
- [5] E. Soleimani-Nasab and M. Uysal, "Generalized performance analysis of mixed RF/FSO cooperative systems," *IEEE Trans. Wireless Commun.*, vol. 15, no. 1, pp. 714-727, Jan. 2016.

- [6] L. Yang, M. O. Hasna, and X. Gao, "Performance of mixed RF/FSO with variable gain over generalized atmospheric turbulence channels," *IEEE J. Sel. Areas Commun.*, vol. 33, no. 9, pp. 1913-1924, Sept. 2015.
- [7] N. Varshney and A. K. Jagannatham, "Cognitive decode-and-forward MIMO-RF/FSO cooperative relay networks," *IEEE Commun. Lett.*, vol. 21, no. 4, pp. 893-896, Apr. 2017.
- [8] N. Varshney, P. K. Sharma, and M.-S. Alouini, "Opportunistic scheduling in underlay cognitive radio based MIMO-RF/FSO networks," arXiv:1805.08943, May 2018, [Online]: <https://arxiv.org/abs/1805.08943>.
- [9] N. Varshney, A. K. Jagannatham, and P. K. Varshney, "Cognitive MIMO-RF/FSO cooperative relay communication with mobile nodes and imperfect channel state information," *IEEE Trans. Cogn. Commun. Netw.*, doi: 10.1109/tccn.2018.2844827, pp. 1-12, Jun. 2018.
- [10] L. Yang, M. O. Hasna, and I. S. Ansari, "Unified performance analysis for multiuser mixed  $\eta$ - $\mu$  and  $\mathcal{M}$ -distribution dual-hop RF/FSO systems," *IEEE Trans. Commun.*, vol. 65, no. 8, pp. 3601-3613, Aug. 2017.
- [11] N. S. Ferdinand, D. B. d. Costa, and M. Latva-aho, "Effects of outdated CSI on the secrecy performance of MISO wiretap channels with transmit antenna selection," *IEEE Commun. Lett.*, vol. 17, no. 5, pp. 864-867, May 2013.
- [12] G. Pan, H. Lei, Y. Deng, L. Fan, J. Yang, Y. Chen, and Z. Ding, "On secrecy performance of MISO SWIPT systems with TAS and imperfect CSI," *IEEE Trans. Commun.*, vol. 64, no. 9, pp. 3831-3843, Sept. 2016.
- [13] L. Fan, X. Lei, N. Yang, T. Q. Duong, and G. K. Karagiannidis, "Secrecy cooperative networks with outdated relay selection over correlated fading channels," *IEEE Trans. Veh. Technol.*, vol. 66, no. 8, pp. 7599-7603, Aug. 2017.
- [14] Z. Wei, D. W. K. Ng, J. Yuan and H. Wang, "Optimal resource allocation for power-efficient MC-NOMA with imperfect channel state information," *IEEE Trans. Commun.*, vol. 65, no. 9, pp. 3944-3961, Sept. 2017.
- [15] R. Zhao, H. Lin, Y.-C. He, D.-H. Chen, Y. Huang, and L. Yang, "Secrecy performance of transmit antenna selection for MIMO relay systems with outdated CSI," *IEEE Trans. Commun.*, vol. 66, no. 2, pp. 546-559, Feb. 2018.
- [16] C. Kong, C. Zhong, M. Matthaiou, E. Bjornson, and Z. Zhang, "Multipair two-way half-duplex DF relaying with massive arrays and imperfect CSI," *IEEE Trans. Wireless Commun.*, vol. 17, no. 5, pp. 3269-3283, May 2018.
- [17] Q. Li and L. Yang, "Artificial noise aided secure precoding for MIMO untrusted two-way relay systems with perfect and imperfect channel state information," *IEEE Trans. Inf. Forensics Security*, vol. 13, no. 10, pp. 2628-2638, Oct. 2018.
- [18] N. Varshney and M. Parul Puri, "Performance analysis of decode-and-forward-based mixed MIMO-RF/FSO cooperative systems with source mobility and imperfect CSI," *J. Lightwave. Technol.*, vol. 35, no. 11, pp. 2070-2077, Jun. 2017.
- [19] A. M. Salhab, "Performance of multiuser mixed RF/FSO relay networks with generalized order user scheduling and outdated channel information," *Arab. J. Sci. Eng.*, vol. 40, no. 9, pp. 2671-2683, Jul. 2015.
- [20] A. M. Salhab, F. S. Al-Qahtani, R. M. Radaydeh, S. A. Zummo, and H. Alnuweiri, "Power allocation and performance of multiuser mixed RF/FSO relay networks with opportunistic scheduling and outdated channel information," *J. Lightwave. Technol.*, vol. 34, no. 13, pp. 3259-3272, Jul. 2016.
- [21] G. T. Djordjevic, M. I. Petkovic, A. M. Cvetkovic, and G. K. Karagiannidis, "Mixed RF/FSO relaying with outdated channel state information," *IEEE J. Sel. Areas Commun.*, vol. 33, no. 9, pp. 1935-1948, Sept. 2015.
- [22] M. I. Petkovic, A. M. Cvetkovic, G. T. Djordjevic, and a. G. K. Karagiannidis, "Partial relay selection with outdated channel state estimation in mixed RF/FSO systems," *J. Lightwave. Technol.*, vol. 33, no. 13, pp. 2860-2867, Jul. 2015.
- [23] E. Balti, M. Guizani, B. Hamdaoui, and B. Khalfi, "Aggregate hardware impairments over mixed RF/FSO relaying systems with outdated CSI," *IEEE Trans. Commun.*, vol. 66, no. 3, pp. 1110-1123, Mar. 2018.
- [24] M. Bloch, J. Barros, M. R. D. Rodrigues, and S. W. McLaughlin, "Wireless information-theoretic security," *IEEE Trans. Inf. Theory*, vol. 54, no. 6, pp. 2515-2534, Jun. 2008.
- [25] L. Fan, X. Lei, N. Yang, T. Q. Duong, and G. K. Karagiannidis, "Secure multiple amplify-and-forward relaying with cochannel interference," *IEEE J. Sel. Topics Signal Process.*, vol. 10, no. 8, pp. 1494-1505, Dec. 2016.

- [26] G. Pan, J. Ye, and Z. Ding, "On secure VLC systems with spatially random terminals," *IEEE Commun. Lett.*, vol. 21, no. 3, pp. 492-495, Mar. 2017.
- [27] G. Pan, J. Ye, and Z. Ding, "Secure hybrid VLC-RF systems with light energy harvesting," *IEEE Trans. Commun.*, vol. 65, no. 10, pp. 4348-4359, Oct. 2017.
- [28] A. H. A. El-Malek, A. M. Salhab, S. A. Zummo, and M.-S. Alouini, "Security-reliability trade-off analysis for multiuser SIMO mixed RF/FSO relay networks with opportunistic user scheduling," *IEEE Trans. Wireless Commun.*, vol. 15, no. 9, pp. 5904-5918, Sept. 2016.
- [29] A. H. A. El-Malek, A. M. Salhab, S. A. Zummo, and M.-S. Alouini, "Effect of RF interference on the security-reliability trade-off analysis of multiuser mixed RF/FSO relay networks with power allocation," *J. Lightwave Technol.*, vol. 35, no. 9, pp. 1490-1505, May 2017.
- [30] H. Lei, Z. Dai, I. S. Ansari, K. H. Park, G. Pan, and M.-S. Alouini, "On secrecy performance of mixed RF-FSO systems," *IEEE Photon. J.*, vol. 9, no. 4, pp. 1-14, Aug. 2017.
- [31] H. Lei, Z. Dai, K.-H. Park, G. Pan, W. Lei, and M.-S. Alouini, "Secrecy outage analysis of mixed RF-FSO downlink SWIPT systems", doi: 10.1109/TCOMM.2018.2865944, May 2018.
- [32] J. Feng and X. Zhao, "Performance analysis of OOK-based FSO systems in Gamma-Gamma turbulence with imprecise channel models," *Opt. Commun.*, vol. 402, pp. 340-348, Nov. 2017.
- [33] H. Lei, H. Luo, K.-H. Park, G. Pan, Z. Ren, and M.-S. Alouini, "On secrecy performance of mixed RF-FSO systems with channel imperfection," *IEEE Photon. J.*, vol. 10, no. 3, pp. 1-14, Jun. 2018.
- [34] A. Jurado-Navas, J. M. Garrido-Balsells, J. F. Paris, M. Castillo-Vázquez, and A. Puerta-Notario, "Further insights on Málaga distribution for atmospheric optical communications," in *Proc. 2012 International Workshop on Optical Wireless Communications (IWOW)*, Pisa, Oct. 2012, pp. 1-3.
- [35] I. S. Ansari, F. Yilmaz, and M.-S. Alouini, "Performance analysis of free-space optical links over Málaga ( $\mathcal{M}$ ) turbulence channels with pointing errors," *IEEE Trans. Wireless Commun.*, vol. 15, no. 1, pp. 91-102, Jan. 2016.
- [36] H. Lei, C. Gao, I. S. Ansari, Y. Guo, Y. Zou, G. Pan, and K. Qaraqe, "Secrecy outage performance of transmit antenna selection for MIMO underlay cognitive radio systems over Nakagami- $m$  channels," *IEEE Trans. Veh. Technol.*, vol. 66, no. 3, pp. 2237-2250, Mar. 2017.
- [37] H. Lei, M. Xu, I. S. Ansari, G. Pan, K. A. Qaraqe, and M.-S. Alouini, "On secure underlay MIMO cognitive radio networks with energy harvesting and transmit antenna selection," *IEEE Trans. Green Commun. Netw.*, vol. 1, no. 2, pp. 192-203, Jun. 2017.
- [38] H. Lei, J. Zhang, K.-H. Park, P. Xu, I. S. Ansari, G. Pan, B. Alomair, and M.-S. Alouini, "On secure NOMA systems with transmit antenna selection schemes," *IEEE Access*, vol. 5, no. 1, pp. 17450-17464, Sept. 2017.
- [39] H. Lei, J. Zhang, K.-H. Park, P. Xu, Z. Zhang, G. Pan, and M.-S. Alouini, "Secrecy outage of Max-Min TAS scheme in MIMO-NOMA systems," *IEEE Trans. Veh. Technol.*, vol. 67, no. 8, pp. 6981-6990, Aug. 2018.
- [40] I. S. Gradshteyn and I. M. Ryzhik, *Table of Integrals, Series and Products*, 7th. San Diego, CA: Academic Press, 2007.
- [41] E. Zedini, H. Soury, and M.-S. Alouini, "On the performance analysis of dual-hop mixed RF/FSO systems," *IEEE Trans. Wireless Commun.*, vol. 15, no. 5, pp. 3679-3689, May 2016.
- [42] E. Zedini, I. S. Ansari, and M.-S. Alouini, "Performance analysis of mixed Nakagami- $m$  and Gamma-Gamma dual-hop FSO transmission systems," *IEEE Photon. J.*, vol. 7, no. 1, pp. 1-20, Feb. 2015.
- [43] Y. Zou, J. Zhu, X. Wang, and V. Leung, "Improving physical-layer security in wireless communications using diversity techniques," *IEEE Netw.*, vol. 29, no. 1, pp. 42-48, Jan. 2015.
- [44] H. Lei, C. Gao, Y. Guo, and G. Pan, "On physical layer security over generalized Gamma fading channels," *IEEE Commun. Lett.*, vol. 19, no. 7, pp. 1257-1260, Jul. 2015.

- [45] V. S. Adamchik and O. I. Marichev, "The algorithm for calculating integrals of hypergeometric type functions and its realization in REDUCE system," in *Proc. the international symposium on Symbolic and algebraic computation (ISSAC '90)*, Tokyo, Japan, Aug. 1990, pp. 212-224.
- [46] E. Zedini, A. Chelli, and M. S. Alouini, "On the performance analysis of hybrid ARQ with incremental redundancy and with code combining over free-space optical channels with pointing errors," *IEEE Photon. J.*, vol. 6, no. 4, pp. 1-18, Aug. 2014.
- [47] N. Yang, P. L. Yeoh, M. Elkashlan, R. Schober, and I. B. Collings, "Transmit antenna selection for security enhancement in MIMO wiretap channels," *IEEE Trans. Commun.*, vol. 61, no. 1, pp. 144-154, Jan. 2013.
- [48] The Wolfram Functions Site. Available: <http://functions.wolfram.com>
- [49] N. Yang, M. Elkashlan, P. L. Yeoh, and J. Yuan, "Multiuser MIMO relay networks in Nakagami- $m$  fading channels," *IEEE Trans. Commun.*, vol. 60, no. 11, pp. 3298-3310, Nov. 2012.